Journal of Magnetic Resonance **137,** 154–160 (1999)
Article ID jmre.1998.1678, available online at http://www.idealibrary.com on IDEAL®

MRI Edge Enhancement as a Diffusive Discord of Spin Phase Structure

Janez Stepišnik,*,† Andrej Duh,‡ Aleš Mohorič,* and Igor Serša†

*Physics Department, University of Ljubljana, Jadranska 19, and †J. Stefan Institute, Jamova 39, 1000 Ljubljana; and ‡Institute of Mathematics and Physics, University of Maribor, Faculty of Electrical Engineering and Computer Science, Smetanova 17, 2000 Maribor, Slovenia

Received July 23, 1998; revised October 30, 1998

The enhancement of magnetic resonance image intensity near impermeable boundaries can be nicely described by a new approach where the diffusional spin echo attenuation is linked to the correlation function of molecular motion. In this method the spin phase structure created by the applied gradient is considered to be a composition of plane waves with the wave vectors representing feasible momentum states of a particle in confinement. The enhancement of edges on the magnetic resonance images (MRI) comes out as a discord of plane waves due to particle motion. It results from the average of the wave phase by using the cumulant expansion in the Gaussian approximation. The acquired analytical expression describes the MRI signal space distribution where the enhancement of edges depends on the intensity and the duration of gradient sequence as well as on the length of the mean squared particle displacement in restricted geometry. This new method works well with gradients of general waveform and is, therefore, suitable for imaging sequences where finite or even modulated gradients are usually used.

Key Words: **NMR; nuclear magnetic resonance; spin echo; magnetic resonance imaging; edge enhancement; gradient; nonuniform field; diffusion; restricted diffusion; velocity correlation; random motion; stochastic; cumulant expansion; Gaussian process; porous system.**

INTRODUCTION

The molecular self-diffusion that tends to attenuate the NMR signal at gradient spin echo is responsible for an edge enhancement effect that may limit the resolution achievable in NMR microscopy. While it is known that motional narrowing due to molecular self-diffusion could cause image blurring at microscopic resolution, the intensity enhancement of MRI is caused by diffusive attenuation (*3–5*) rather than by diffusive lineshape distortion (*6, 7*) or enhancement of magnetization near barriers (*8*). Namely, the spin echo signal exhibits weaker diffusion attenuation at boundaries since the motion is restricted by walls. Thus, in certain circumstances, the edges of a region may be enhanced in MR images. This was experimentally confirmed by Callaghan *et al.* (*5*) and others. In attempts to provide an extensive quantitative theory Hyslop *et al.* (*3*) and de Swiet *et al.* (*4, 9*) have used the Torrey–Bloch (*10*) equation to define characteristic regimes of observation. These are regimes of the slow and fast exchange of spin compared to the time of signal acquisition. Callaghan and Codd (*11*) employed an impulse-propagator method with matrix multiplication to calculate edge effects on the NMR image.

Generally, the calculation of image contrast and other distortion effects arising from these phenomena is not at all quite simple. As yet there is no general analytic expression that would describe thoroughly the effect and work for an imaging pulse sequence with gradient pulses of general form. This paper is an attempt to tackle diffusive MRI edge distortion by the recently developed theory of gradient spin echo attenuation of restricted diffusion (*2, 12*). Preliminary results (*13, 14*) indicate this could solve the problem of providing the MRI diffusion edge enhancement in analytic form for a general imaging sequence.

In this theory we consider the spin phase distribution created by an applied gradient within the enclosed volume of a pore,

$$\theta_i(t) = \mathbf{F}(t)\cdot\mathbf{r}_i(t) - \int_0^t \mathbf{F}(t)\cdot\mathbf{v}_i(t)dt, \qquad [1]$$

where $\mathbf{F}(t) = \gamma\int_0^t \mathbf{G}(t)dt$ and $\mathbf{v}_i(t)$ is particle velocity. Owing to molecular confinement in the pore, the spin phase factor can be described as a composition of a series of plane waves,

$$e^{i\mathbf{F}\mathbf{r}} = \sum_k S_{\mathbf{k}}(\mathbf{F})e^{i\mathbf{k}\mathbf{r}}, \qquad [2]$$

with the wave vectors $\mathbf{k}$ related to feasible momentum states of particles in confinement.

Random motion of spin-bearing particles in the magnetic field gradient causes a variation of spin precession frequency. By NMR one cannot detect the magnetization of an individual molecule undergoing Brownian motion but rather the induction signal created by innumerable spins. The spin echo is the cumulative effect of a large number of small perturbations of spin precession frequency caused by molecular motion in the

1090-7807/99 $30.00

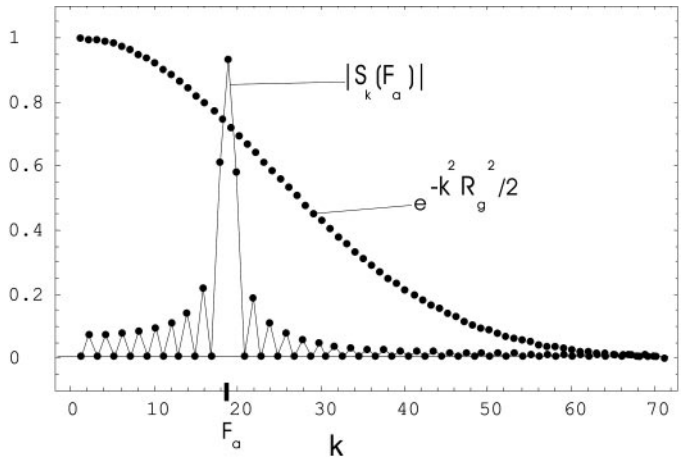

FIG. 1. Structure components and the attenuation factor in plan-parallel confinement.

magnetic field gradient. Consequently, it is possible to apply the central limit theorem and consider detected frequency fluctuation to be a Gaussian random process (*15*), even assuming that the frequency variation of an individual spin might behave as a non-Gaussian process. Thus the ensemble average with the cumulant expansion (*1, 2*) gives the signal at the peak of spin echo as

$$E(\mathbf{F}_a, \tau) = \int_V E_o(\mathbf{r}) e^{i\mathbf{F}_a(t)\mathbf{r}} \sum_{\mathbf{k}} S_{\mathbf{k}}(\mathbf{F}_a) e^{-i\mathbf{k}\cdot r} e^{-(1/2)\mathbf{k}^2 \cdot R_g^2(\tau,\mathbf{r})} d\mathbf{r}. \quad [3]$$

The acquired expression comprises the components of phase structure, $S_{\mathbf{k}}(\mathbf{F}_a)$, attenuated by factors depending on the diffusion length of the particle at the location $\mathbf{r}$ in the restricted geometry $R_g^2(\tau, \mathbf{r})$. We have introduced two new quantities (*2*) having the following meanings:

1. A sequence of gradient pulses creates an average spin dephasing of moving spin particles as

$$\mathbf{F}_a(\tau) = \frac{\mathbf{f}}{R_{gi}(\tau)} \sqrt{\int_0^\tau \int_0^\tau \mathbf{F}(t_1) \langle \mathbf{v}_i(t_1) \cdot \mathbf{v}_i(t_2) \rangle_c \mathbf{F}(t_2) dt_1 dt_2}, \quad [4]$$

where the unit vector $\mathbf{f}$ is aligned along the direction determined by the cumulative effect of applied gradients and where v_{gi} denotes the velocity of the ith particle along the directions of applied gradients. Namely, due to a finite (or modulated) gradient waveform (which may change direction), the spin phase structure is not created in a step, as in the case of short pulse gradients, but is built up during an extended interval of gradient persistence. Clearly, the formation of nonuniform spin phase structure is accompanied by particle motion tending to destroy its buildup. Thus the gradient/velocity correlation function in the phase integral, Eq. [4], hides two processes with opposite tendencies. In the case of a spin echo sequence with a short enough duration so that most of the particles do not reach the boundaries, $\mathbf{F}_a$ can be approximated as a spin dephasing in an unbounded medium. For an isotropic liquid and short correlation times $\tau_c \ll \tau$ it is equal to

$$\mathbf{F}_a(\tau) = \frac{\mathbf{f}}{\tau} \sqrt{\int_0^\tau \mathbf{F}(t)^2 dt}. \quad [5]$$

In the special case when two gradient pulses of duration δ separated by time Δ are applied,

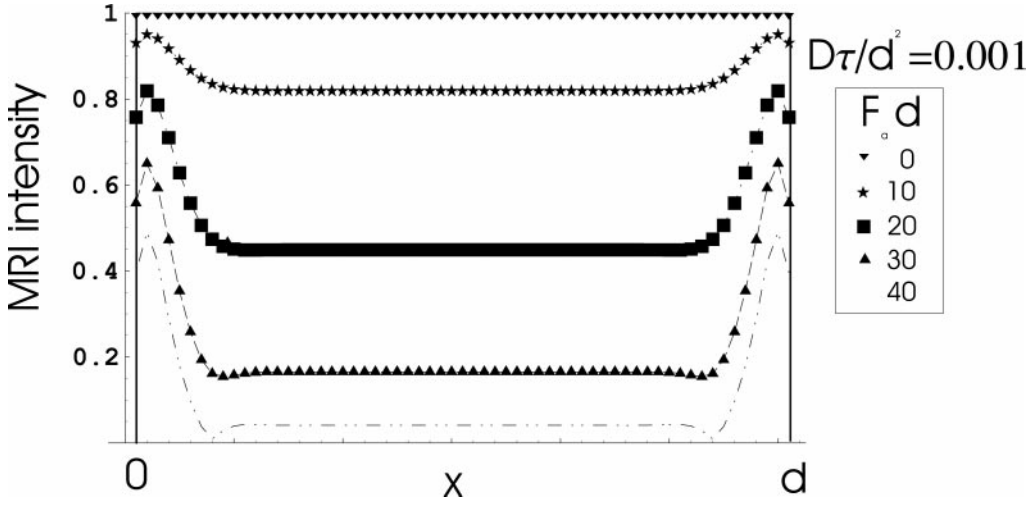

FIG. 2. Calculated one-dimensional MR image of spins enclosed by plan-parallel walls. Edge enhancement at constant diffusion time remains almost unchanged in a broad range of F_a variation.

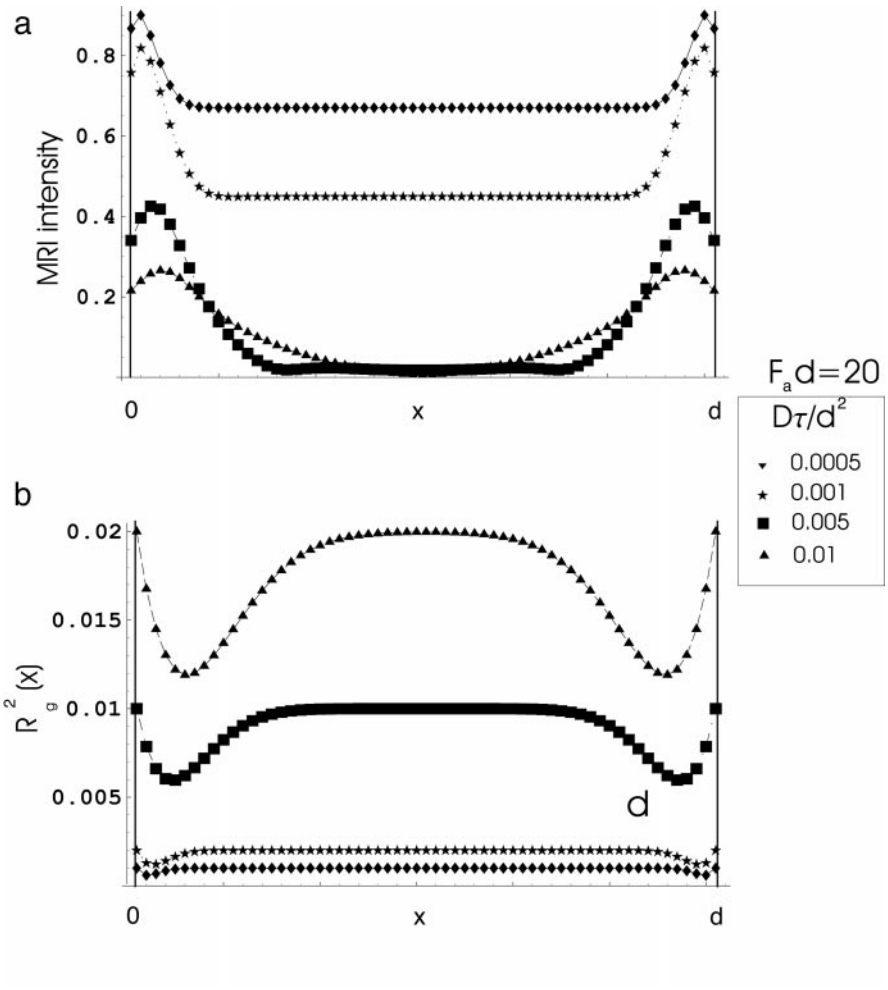

FIG. 3. (a) Calculated one-dimensional MR image of spins enclosed by plan-parallel walls for different diffusion times τ at the constant spin dephasing F_a. (b) The mean-square particle displacement, $R_g(x)$, dependence on the initial location of particle in the cell which is approximated with the help of joint probability function from Fick's law.

$$|\mathbf{F}_a(\tau)| = \gamma G \delta \sqrt{\frac{\Delta - \delta/3}{2\Delta}}.$$

$\mathbf{F}_a(\tau)$ in the general form of Eq. [4] includes all regimes of motion including the transition from the regime of slow to fast exchange of spins, as defined in Refs. (*3*) and (*9*). However, Eq. [4] shows that knowledge of a diffusion constant/gradient amplitude ratio is not enough to reveal all features in these regimes. Whenever the signal sampling is accompanied by substantial diffusion shifts of molecules in the restricted region, details of molecular motional correlation, $\langle v_{gi}(t_1) \cdot v_{gi}(t_2)\rangle_c$, must be known.

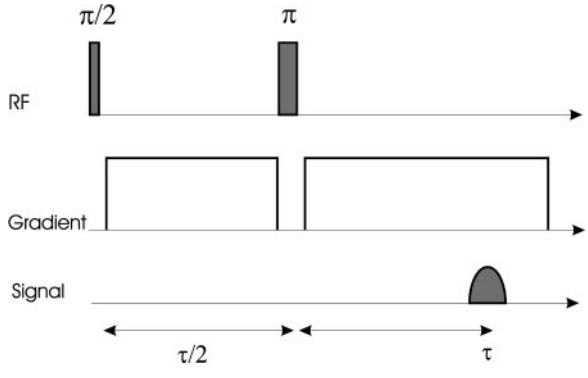

FIG. 4. MRI pulse sequence.

2. The mean squared particle displacement along the applied gradient, $R_g^2(\tau, \mathbf{r})$, depends on duration and directions of applied gradients as well as on the averaged location of the particle in the pore, $\mathbf{r}$. For an infinite system the velocity correlation is positive and falls off quickly with time. Thus for times longer than the correlation time, $\tau \gg \tau_c$, the diffusion length is

$$R_g(\tau)^2 = 2D_g\tau, \qquad [6]$$

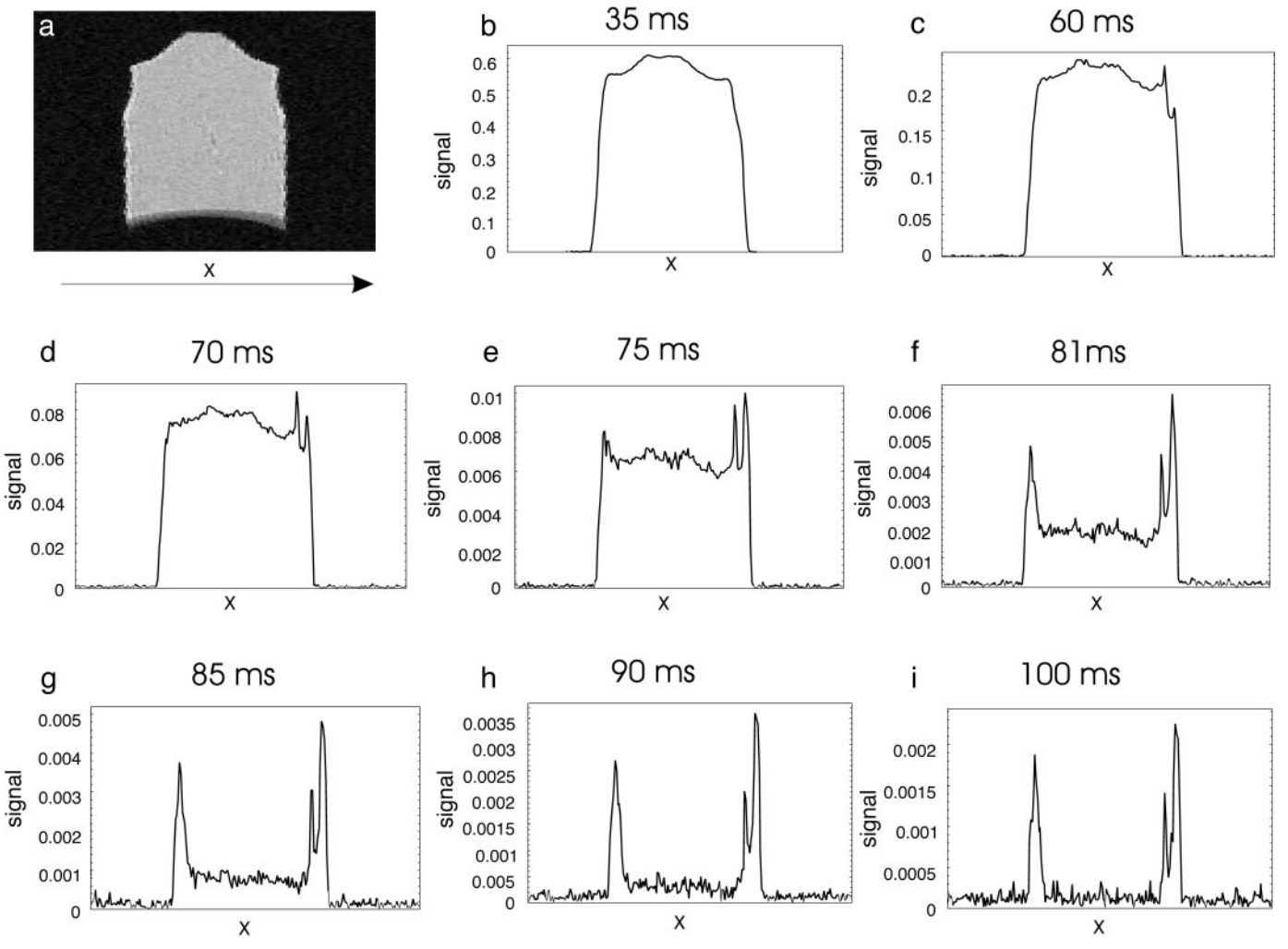

FIG. 5. (a) MRI of water in the notch in the transverse cross-section. Image is extended along the *x* axis to amplify view of edges. (b)–(i) Their one-dimensional projections at the acquisition times varying from 35 to 100 ms.

where D_g is an average diffusion rate along the directions of spin dephasing. In the case of confined diffusion the velocity correlation function cannot be approximated as a δ function but as a function depending on the size of the pore and the scattering mechanism of molecules at the walls (*16–18*). Therefore, in the regime of fast spin exchange, when particles frequently collide with walls, a more generalized form of diffusion length has to be taken into account,

$$R^2_{gi}(\tau) = \int_0^\tau \int_0^\tau \langle v_{gi}(t_1) \cdot v_{gi}(t_2) \rangle_c \, dt_1 dt_2, \qquad [7]$$

where the velocity correlation function holds details of the molecular motion and the scattering process.

As yet we based the arguments for usage of Gaussian approximation on the central limit theorem, but it is important to note that evidence follows from the estimate of cumulant series convergence (*19*) as well. When assuming that the correlation time, τ_c, corresponding to the average collision time of molecules, is much shorter than the spin echo pulse sequence τ, the evaluation of higher order velocity correlation gives *n*-term of cumulant series roughly linear in time. Its magnitude appears to be proportional to *n*th power of spin phase fluctuation as $(F_a l)^n$, where l is a molecular mean free path. It provides, for instance in the case of the two gradient pulse sequences with pulse width δ, that all cumulants higher than the second order can be omitted (and fluctuations considered Gaussian random process) when $\gamma G \cdot \delta \ll 1/l$.

MRI EDGE ENHANCEMENT BY MOLECULAR DIFFUSION

The main advantage of this theory over other approaches is its ability to incorporate very general pulse sequences where a

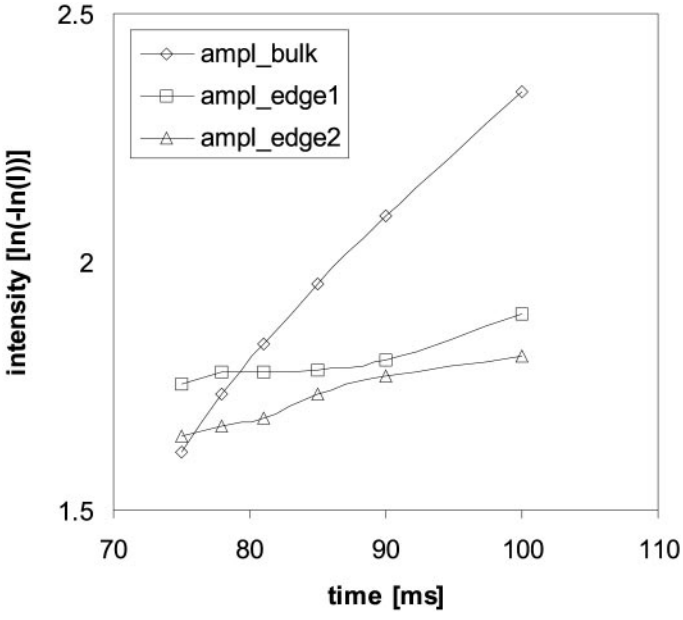

FIG. 6. Intensities of various sections of one-dimensional MR images as a function of signal acquisition time.

finite-width or even modulated gradient pulses are used. Thus we expect it could adequately describe the MRI diffusive artifact that appears at edged structures or other diffusion phenomena arising at NMR microscopy of a porous structure.

If we assume that the data acquisition interval, Δt, is short enough compare to the inverse rate of diffusion attenuation, $\Delta t \ll 1/F_a^2 D$, then the magnitude of NMR signal induced by ensemble spins can be written as

$$|e(\mathbf{r}, \mathbf{F}_a, \tau)| = |e(\mathbf{r})_0 \sum_{\mathbf{k}} S_{\mathbf{k}}(\mathbf{F}_a) e^{i\mathbf{k}\mathbf{r}} e^{-(1/2)\mathbf{k}^2 R_g^2(\tau, \mathbf{r})}|. \quad [8]$$

Here we neglect the spin relaxation and r denotes the mean location of a spin-bearing particle. Figure 1 exposes terms of this equation presented in the reciprocal space. The components of the phase structure $S_{\mathbf{k}}(\mathbf{F}_a)$ are symmetrically distributed around the point $\mathbf{k} \approx \mathbf{F}_a$. In the sum [8], each term is reduced for an attenuation factor $e^{-(1/2)\mathbf{k}^2 R_g^2(\tau,\mathbf{r})}$. In Eq. [8] the predominating structure component $S_{\mathbf{k}\approx\mathbf{F}_a}(\mathbf{F}_a)$, experiencing the attenuation of $e^{-(1/2)\mathbf{F}_a^2 R_g^2(\tau,\mathbf{r})}$, appertains to the spin dephasing in the bulk. The attenuation strengthens for components with $\mathbf{k} > \mathbf{F}_a$ and lessens when lowering $\mathbf{k}$. Thus there is almost no attenuation for components close to $\mathbf{k} = 0$. Along this line follows the basic understanding of the MRI contrast enhancement at edges. The component with $\mathbf{k} \approx \mathbf{F}_a$ that belongs to spins in the bulk experiences usual Torrey's diffusion attenuation, while those in the vicinity of $\mathbf{k} \approx 0$ represent almost unspoiled signal induced by spins at the proximity of compartment walls. This asymmetric attenuation of spin phase structure components brings about an apparent increase of MRI signal at the edges while reducing the intensity of the bulk-spin signal.

In the following we will restrain our consideration to a simple sequence where the magnetic field gradient is aligned only in one direction, although the method is very general and capable of explaining the effect when very sophisticated imaging sequences are applied. One-dimensional images of water spins closed between parallel walls will reveal interesting details of phenomena relevant for images obtained from the spins in the confinement of more general geometry. The magnitude of the MRI signal induced by spins in a pixel at x follows from Eq. [8] as

$$|e(x, F_a, \tau)| = |e(x)_0 \sum_{n=-\infty}^{\infty} S_n(F_a) e^{i(n\pi/d)x} e^{-(1/2)(n\pi/d)^2 R_g^2(\tau,r)}| \quad [9]$$

with

$$S_n(F) = i \frac{(Fd + n\pi)e^{iFd} - (-1)^n 2Fd + (Fd - n\pi)e^{iFd}}{(-1)^n 2(n^2\pi^2 - F^2 d^2)}, \quad [10]$$

where R_g^2 is a mean-square displacement along the gradient aligned in the direction of x axes perpendicular to the plane boundaries. Figure 2 shows one-dimensional NMR image of spins in a slit calculated according to Eq. [9]. The increase of spin dephasing F_a intensifies the image contrast in proximity to compartment walls ($x = 0$ and $x = d$). It appears as broadened lines truncated at the edges ($x = 0$ and d) and with the peaks shifted from the proximity of the edges. The width of lines and position of peaks do not change with increasing F_a.

By changing the time of π RF pulse application we can alter the time of molecular diffusion at unchanged F_a. Resulting variations of the edge enhancement are shown in Fig. 3. In the short-time approximation the exact calculation of a mean velocity correlation function for diffusion between plan-parallel planes (*20*) gives the same result as that obtained according to Fick's law (*21*). Therefore, we adopt position-dependence of mean squared displacement as calculated with the conditional probability according to the diffusion law, Fig. 3b. Doing so demonstrates that for molecules in proximity to walls, the mean squared displacement of molecules is shorter than in the bulk. Prolonging the diffusion time moves the shortest displacement away from the walls and causes a shift of the enhanced line peaks away from the wall edges. The line shift is accompanied by line broadening, which is proportional to a mean diffusion length as $R_g \approx 2D\tau$. Thus at longer time intervals the intensity reduction of the enhanced line should follow a linear dependence on time.

EXPERIMENT AND DISCUSSION

In order to test theoretical features of the diffusion edge enhancement, Eq. [9], presented in Figs. 2 and 3, we have prepared a sample of water contained in a narrow notch milled in a piece of plastic. The notch was 29 mm long and shaped as the milling knife in the transverse section, Fig. 5a. There are two different widths of the notch: the 4.5-mm-deep lower part had a width of 2.8 mm while the 2.5-mm-long neck had a width of 2.6 mm. The bottom of the notch had a 1.5-mm-deep cone shape of the milling knife.

The experiment was carried out using an NMR imager with a 3-T superconductive magnet with probe incorporating a quadrupolar coil able to produce a magnetic field gradient of 0.03 T/m. Images were taken by sampling 512 points at intervals of 60 μs with total duration about 31 ms; see Fig. 3. One-dimensional NMR imaging was carried out with the slit carefully aligned so that the magnetic field gradient direction was as nearly normal as possible to the wall of the slit. An ordinary spin echo sequence with two long gradient pulse was used, Fig. 4, in which the second gradient pulse was prolonged to sample the signal for one-dimensional MRI. In order to get the MRI at different diffusion times, we changed the duration of the first gradient pulse. Thus, the sampling interval that remained unchanged was moving from 30 to 100 ms.

The transverse section of the MR images, Fig. 5, clearly shows distinct two-edge enhancement of two different widths of the notch. The enhancement is more pronounced on the right-hand side of the one-dimensional MR images. Although the edges were only 0.1 mm apart, the resolution seems to be better than 0.05 mm. The enhancement on the left-hand side of the image is less distinctive and two-edge enhancement is blurred into one line. By turning the sample in the probe for 180°, the lines on the left side remained mingled while the enhancements on the right-hand side appeared distinctive again. We believe that the line blurring, which appears only on one side of the images, is due to the gradient nonlinearity along the length of the notch. Therefore we have limited further analysis only to the lines of well-distinguished edges.

For sampling at times 60 and 70 ms, two distinct and well-separated narrow lines clearly indicate the proper distance between two edges. The lines partly overlap when the sampling interval is moved to the times between 81 and 100 ms. According to the theoretical prediction shown in Fig. 3, a prolongation of the diffusion length R_g broadens the line of enhancement. This is proven by the experiment where edge enhancement was observed in MRI of hyperpolarized ^{3}He (*22*). There rapid gas diffusion extends the range of edge enhancement far away from the boundaries. In our experiments the molecular diffusion time changes from 30 to 100 ms, which gives mean particle displacements, $\sqrt{2D\tau}$, ranging from about 0.012 to 0.022 mm. This brings about partial overlapping of two-edge lines; Figs. 5d, 5e, and 5f. Although the resolution of our imager limits accurate quantitative determination of the line broadening, it can be obtained by following the change of line intensities as they decrease in proportional to line broadening, Fig. 3. Figure 6 shows the experimental results of edge enhancement. The intensities of enhanced lines from the right-hand side of MR images and the intensity of the middle part of the image are shown on a log–log plot as a function of time. According to the slopes, the attenuation of bulk signal decreases to τ^3, while, after reaching the maximum at about 70 ms, the lines of enhanced edges follow almost a linear dependence on the diffusion time. This agrees with the calculations from Eq. [9], where the intensity of enhanced lines is lower due to the line broadening, which is proportional to the mean square of particle displacement $2D\tau$.

CONCLUSION

Equation [8] describes the artifact of NMR microscopic imaging known as an intensity enhancement due to the restraint of molecular motion in the proximity of boundaries. We derived it by averaging the spin phase and expanding a nonuniform spin phase distribution into a series of plane waves. Their wave vectors represent feasible momentum states of particles within confinement and, thus, characterize the geometry and boundaries of confinement. Random motion brings about a discord of structure waves and disrupts the initial phase structure. The spatially nonuniform intensity distribution of the NMR signal is due to weaker spin echo attenuation at the confinement boundaries.

The result of a new approach is the analytic description of the effect, Eq. [8], that can be used to image sequences with gradient pulses of finite width and general waveform. But in order to anticipate the exact form of edge enhancement, one must know the position dependence of mean squared particle displacement within the pore. Nevertheless the problem can be turned upside down: With the use of the high-resolution NMR imager we can implement the method to bring to light the information about mean squared displacement and thus about molecular motional correlation in confined geometry.

It seems that good agreement between the experimental results and the evaluation can serve as a confirmation of the basic assumptions of the new approach.

REFERENCES

1. J. Stepišnik, *Physica B* **104,** 350–364 (1981).
2. J. Stepišnik, *J. Magn. Reson.* **131,** 339–346 (1998).
3. B. W. Hyslop and P. C. Lauterbur, *J. Magn. Reson.* **94,** 501–510 (1991).
4. T. M. de Swiet and P. N. Sen, *J. Chem. Phys.* **100,** 5597–5604 (1994).
5. P. T. Callaghan, A. Coy, L. C. Forde, and C. J. Rofe, *J. Magn. Reson. A* **101,** 347–350 (1993).
6. B. Putz, D. Barsky, and K. Schulten, *Chem. Phys. Lett.* **183,** 391–396 (1991).

7. B. Putz, D. Barsky, and K. Schulten, *J. Magn. Reson.* **976,** 27–53 (1992).

8. D. Barsky, B. Putz, K. Schulten, J. Schoeniger, E. W. Hsu, and S. Blackband, *Chem. Phys. Lett.* **200,** 88–96 (1992).

9. T. M. de Swiet, *J. Magn. Reson. B* **109,** 12–18 (1995).

10. H. C. Torrey, *Phys. Rev.* **104,** 563–565 (1956).

11. P. T. Callaghan and S. L. Codd, *Magn. Reson. Imaging,* in press (1998).

12. J. Stepišnik, "28th Congress Ampere, Canterbury," Book of extended abstracts, 91–92 (1996).

13. J. Stepišnik and A. Duh, "13th European Experimental NMR Conference," Book of abstracts, p. 361 (1996).

14. A. Duh and J. Stepišnik, "4th International Conference on Magnetic Resonance Microscopy and Macroscopy," Book of abstracts, p. 112 (1997).

15. N. G. van Kampen, "Stochastic Processes in Physics and Chemistry." North-Holland, Amsterdam (1981).

16. A. Rahman, *Phys. Rev. A* **136,** 405–411 (1964).

17. D. Levesque and L. Verlet, *Phys. Rev. A* **2,** 2514–2528 (1970).

18. P. Grassberger, *Physica A* **103,** 558–572 (1980).

19. J. Stepišnik, *Physica B,* in press (1999).

20. E. Oppenheim and P. Mazur, *Physica* **30,** 1833–1845 (1964).

21. J. Stepišnik, *Physica B* **198,** 299–306 (1994).

22. B. Saam, N. Drukker, and W. Happer, *Chem. Phys. Lett.* **263,** 481–487 (1996).